Michalowski, R. L. (1995). *Géotechnique* **45**, No. 2, 283–293

Slope stability analysis: a kinematical approach

R. L. MICHALOWSKI*

A stability analysis of slopes based on a translational mechanism of failure is presented. The collapse mechanism is assumed to be in the form of rigid blocks analogous to slices in traditional slice methods. The proposed analysis, although based on the kinematical approach of limit analysis, always satisfies the equilibrium of forces acting on all blocks in the selected mechanism. All slope stability analyses based on the limit equilibrium of slices can be interpreted in the context of their implicitly assumed collapse mechanisms. The static assumptions made are equivalent to assuming an arbitrary strength of the soil on interfaces between slices. Solutions to stability factor $\gamma H/c$ from all analyses based on the limit equilibrium of slices fall into a relatively narrow range bounded by the solutions using the proposed analysis for two extreme assumptions of soil strength between the blocks. Solutions beyond this range obtained by any method of slices indicate unreasonable consequences when interpreted in the context of the failure mechanism. A convenient way to include pore pressure effects is also presented and implemented in the analysis of both translational and rotational slope collapse.

KEYWORDS: embankments; failure; limit state analysis; plasticity; pore pressures; slopes.

L'article présente une analyse de la stabilité des pentes fondée sur des mécanismes de rupture par translation. Le mécanisme de l'effondrement est géré par des blocs rigides, équivalents aux tranches des méthodes traditionnelles. Cette analyse, bien que fondée sur une approche cinématique des analyses aux états limites, vérifie toujours l'équilibre des forces agissant sur l'ensemble des blocs. Toute analyse de la stabilité des pentes fondée sur un équilibre limite des tranches peut être interprétée suivant les mécanismes d'effrondrement qui lui sont implicitement affectés. Les hypothèses statiques posées lors de ces analyses reviennent à supposer l'existence d'une résistance arbitraire du sol au niveau des contacts entre tranches. Les facteurs de stabilité, $\gamma H/c$, calculés à l'aide des différentes analyses par équilibre limite des tranches, sont compris dans un intervalle relativement étroit dont les bornes sont les valeurs obtenues à l'aide de l'analyse proposée pour deux hypothèses extrêmes de résistance du sol entre les blocs. Les valeurs, calculées par n'importe quelle méthode des tranches, situées hors de cet intervalle donnent des résultats aberrants en terme de mécanismes de rupture. Une méthode simple de prise en compte des effets de la pression interstitielle est également présentée puis implémentée dans l'analyse de l'effondrement des pentes par translation et par rotation.

INTRODUCTION

Despite the development of numerical methods for the analysis of slopes, traditional techniques based on the division of the soil mass into slices are still routinely used to evaluate the safety of slopes. The first method of slices for slope stability analysis (Fellenius, 1927) was based more on engineering intuition than on a rigorous mechanics approach. Development of slice methods in the 1950s and 1960s focused on interslice forces and satisfying three equations of equilibrium for each slice (Bishop, 1955; Janbu, 1957, 1973; Morgenstern & Price, 1965; Spencer, 1967). As the original problem was statically indeterminate, some static assumptions had to be made. Satisfying three equations of equilibrium for each slice (two-dimensional deformation problem) did not remove the approximate character of the slice method. Still, no proof was required that a statically admissible stress field exists within the slices and beyond, or that assumed mechanisms of failure are kinematically admissible. The issue of the kinematical admissibility of the failure patterns selected was not even raised, as slice methods do not make use of the stress–strain rate relation. The term 'rigorous' as applied to slice methods needs to be interpreted as the method satisfying the global equilibrium of each slice without violating the yield condition of the soil, and not one that leads to the true stress and

Manuscript received 26 January 1993; revised manuscript accepted 3 June 1994.
Discussion on this Paper closes 1 September 1995; for further details see p. ii.
* Johns Hopkins University, Baltimore.

strain (or strain-rate) fields. Due to arbitrary static assumptions the rigorous slice techniques do not yield a unique solution to the factor of safety.

None of the slice techniques can be considered exact, and it is only a hypothesis based on intuition that the methods satisfying three equations of global equilibrium are more accurate than those that satisfy only one or two. As neither the static admissibility of the stress field nor the kinematic admissibility of the collapse mechanism can be proved for any of the slice methods, such a hypothesis is rather arbitrary. Evaluating which of the slice techniques is more appropriate than the others is not possible without resort to a technique that would at least yield a strict bound to the true solution. The upper bound technique of limit analysis is used in this Paper. This technique was used earlier in the two-dimensional analysis of rotational collapse of slopes (Chen, Giger & Fang, 1969), and it was suggested that it be used with translational mechanisms (Karal, 1977; Izbicki, 1981). More recently this technique was applied in the three-dimensional analysis of locally loaded slopes (Michalowski, 1989). In its theoretical aspect, this analysis is similar to the analyses by Chen *et al.* (1969), Karal (1977) and Izbicki (1981). However, these analyses differ in collapse mechanisms and analytical formulation. In addition, the method presented here explicitly includes the effect of the pore pressure through energy terms.

The object of this Paper is twofold: to present a kinematical limit analysis for assessing the safety of slopes or their critical heights, and to interpret traditional slice methods in terms of their implicitly assumed kinematics in order to indicate the significance of arbitrary static assumptions.

Criticism of traditional slice techniques does not affect their usefulness in practical calculations. It is believed that pointing to the weaknesses of these techniques will lead to a better understanding of the existing methods, and perhaps new methods will emerge. Slice techniques are used successfully in other branches of engineering. A differential slice approach was used in calculations of pressure on silo walls as early as 1895 (Janssen, 1895; Drescher, 1991). Similar techniques are used in metal mechanics, and also appear to be useful in geotechnical analyses in problems other than those of slopes (Janbu, 1957; Michalowski, 1984).

The upper bound technique is reviewed briefly and an admissible slope collapse mechanism associated with traditional slice analyses is presented. A factor of safety for slopes is then derived, based on the upper bound approach used with the failure mechanism of a sliced soil mass. A proposal for including the pore pressure effect is presented, and results of calculations are given.

UPPER BOUND APPROACH

It is assumed that the soil is perfectly plastic, its yield condition is convex in the stress space, and it obeys the associative flow rule

$$\dot{\varepsilon}_{ij} = \dot{\lambda}\, \partial f(\sigma_{ij}')/\partial \sigma_{ij}', \quad \dot{\lambda} \geqslant 0 \tag{1}$$

where $\dot{\varepsilon}_{ij}$ is the strain rate tensor of the soil skeleton, σ_{ij}' is the tensor of effective stress, $f(\sigma_{ij}') = 0$ is the yield condition, and $\dot{\lambda}$ is a non-negative multiplier. The approach is based on using the upper bound theorem, which states that the rate of work done by the external forces (surface tractions and material weight) is less than or equal to the rate of the energy dissipation in any kinematically admissible velocity field. This can be written as

$$\int_v \sigma_{ij}^* \dot{\varepsilon}_{\delta ij}^*\, \mathrm{d}v \geqslant \int_s T_i V_i\, \mathrm{d}s + \int_v X_i V_i^*\, \mathrm{d}v \tag{2}$$

where $\dot{\varepsilon}_{ij}^*$ is the strain rate in the kinematically admissible velocity field, $\dot{\varepsilon}_{ij}^* = (V_{i,j}^* + V_{j,i}^*)/2$, $V_i^* = V_i$ on boundary s (given boundary condition), σ_{ij}^* is the effective stress tensor associated with ε_{ij}^*, X_i is the vector of distributed forces (weight, buoyancy and seepage forces), and s and v are the loaded boundary (surface) and the volume respectively. Thus, equating the energy dissipation rate to the work of the external forces in any admissible failure mechanism will lead to a limit load that is not lower than the true limit load. This is true when the unknown load T_i is active ($T_i V_i > 0$ on boundary s), and such calculation is possible when V_i is constant on s. Alternatively, as in the case of slopes where the tractions are given, the factor of safety defined as

$$F = \frac{c}{c_\mathrm{d}} = \frac{\tan \phi}{\tan \phi_\mathrm{d}} \tag{3}$$

can be calculated using the kinematical approach of limit analysis. Introducing the factor of safety as in equation (3) implies that the slope material obeys the Mohr–Coulomb yield condition. Parameters c and ϕ are the cohesion and internal friction angle, and c_d and ϕ_d are their values necessary to maintain energy balance in an admissible failure mechanism.

The flow rule in equation (1) associated with the Mohr–Coulomb yield condition imposes certain constraints on the kinematics of the collapse mechanism. In particular, the soil becomes dilatant, i.e. its volume increases (density decreases) during deformation. In cases where

velocity discontinuities occur (e.g. in rigid-block mechanisms), the velocity jump vector must be inclined to the discontinuity at the angle of internal friction. The rate of energy dissipation per unit of area of a velocity discontinuity surface (often also called a rupture or a failure surface) for the Coulomb material can be written as

$$\dot{d} = \sigma_{ij}' n_j [V]_i = c[V] \cos \phi \qquad (4)$$

where n_j is the unit vector perpendicular to the rupture surface, $[V]_i$ is the velocity jump vector and $[V]$ is its magnitude. Subscripts i and j in equation (4) denote the Cartesian co-ordinates. The non-associative flow rule for soils can be accounted for in the stability analysis using a technique proposed by Drescher & Detournay (1993).

It should be emphasized that an upper bound solution to a limit load (or a factor of safety) based on a rigid-block translational mechanism yields a solution identical to that of the limit equilibrium method based on the same discrete failure pattern (Mróz & Drescher, 1969). By the principle of virtual work a system of blocks is in equilibrium provided the virtual work done by all external forces and couples is equal to the energy dissipated for each and every virtual displacement of the system consistent with the constraints. Equating the energy dissipation rate to work rate by external forces in a translational mechanism must therefore lead to a solution where the equilibrium of forces is satisfied.

ADMISSIBLE FAILURE MODES ASSOCIATED WITH SLICE ANALYSES

To select a kinematically admissible failure pattern, the flow rule of the soil must be known first. Although the location of the failure surface must be selected in slice techniques (arbitrarily or through a process of minimization of the factor of safety), the entire failure mechanism is not assumed explicitly. Slice techniques make no use of the flow rule, as the considerations are restricted to the equilibrium of forces. To interpret the slice approach in terms of the implicit kinematics it is assumed, as in limit analysis, that the soil obeys the flow rule associated with the Mohr–Coulomb yield condition. Fig. 1(a) shows a typical division of the soil mass into blocks (slices). The failure surface ABCD may be of arbitrary shape.

The division into blocks in the failure mechanism is purposely assumed so that the blocks coincide with the slices considered in traditional analyses. The geometry of each block is characterized by the length of the base l, the inclination angle of the base α, and the lengths of interfaces t (Fig. 1(b)). Block 1 can slide only up or down along base AB. AB, BC, and so on are approximated with plane surfaces. The reasonable direction of movement during failure is down. The associative flow rule requires that the velocity of block 1 be inclined to AB at angle ϕ. For the same reason, the adjacent block must move with a velocity inclined at ϕ to BC. The two blocks then move with different velocities, $[V]$ being the velocity difference (jump) between the two (Fig. 1(c)). If the velocity of the first block is given, the velocities of all blocks can be found by using the hodograph in Fig. 1(d) repeatedly.

Such a mechanism is translational and not rotational. The rigid rotation mechanism is admissible only if the failure surface is a log-spiral (cylindrical surface for frictionless soil). In a mechanism based on blocks as in Fig. 1(a), the energy is dissipated not only along the failure line ABCD, but also within the sliding mass, along the vertical interfaces.

The hodograph for the failure mechanism from Fig. 1(a) is shown in Fig. 2(a). The velocity of the first block is $V_1 = V_0/\sin(\alpha_1 - \phi_1)$, where V_0 is the vertical component of the velocity of the first block (boundary condition). The respective velocities of other blocks V_k and the interfacial

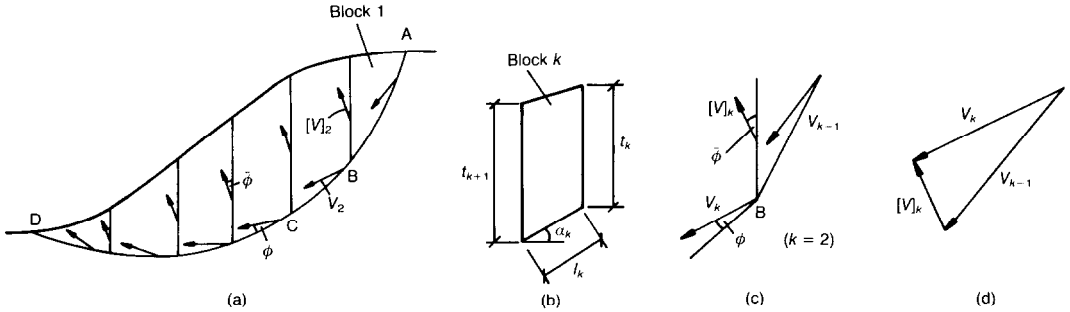

Fig. 1. (a) Translational failure mechanism; (b) single block; (c) velocity vectors; (d) hodograph

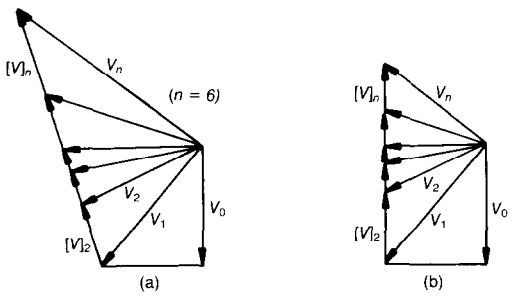

Fig. 2. (a) Hodograph for a homogeneous slope; (b) hodograph when the internal friction on interfaces between blocks is neglected

velocity jumps $[V]_k$ for a convex slip surface are

$$\left.\begin{aligned} V_k &= V_{k-1}\frac{\cos(\alpha_{k-1}-\phi_{k-1}-\bar{\phi}_k)}{\cos(\phi_k+\bar{\phi}_k-\alpha_k)} \\ [V]_k &= V_k\frac{\sin(\phi_k-\phi_{k-1}-\alpha_k+\alpha_{k-1})}{\cos(\alpha_{k-1}-\phi_{k-1}-\bar{\phi}_k)} \end{aligned}\right\} \quad (5)$$

where the subscript k denotes the block number, α_k is the angle of inclination of the block base to the horizontal, ϕ_k is the internal friction angle at the base of the block and $\bar{\phi}_k$ is the internal friction angle on the right interface of the kth block (the interface between blocks k and $k-1$). For a uniform value of ϕ within the soil mass the end points of block velocity vectors are located on one straight line (Fig. 2(a)). When the internal friction angle is different on different surfaces between blocks, these vector end points are not located on a straight line, but equations (5) are still valid.

FACTOR OF SAFETY FOR TRANSLATIONAL COLLAPSE MECHANISMS IN THE ABSENCE OF PORE PRESSURE

Denoting the weight of block k as G_k, and any additional vertical load on the block as Q_k, the rate of work of all forces G_k and Q_k can be written as

$$\dot{W}_\gamma = \sum_{k=1}^{n}(G_k+Q_k)V_k\sin(\alpha_k-\phi_k) \quad (6)$$

where n is the number of blocks. In a rigid-block mechanism as in Fig. 1(a) the energy is dissipated along the failure surface ABCD and on vertical block interfaces. With reference to equation (4), the energy dissipation rate in the entire mechanism becomes

$$\dot{D} = \sum_{k=1}^{n}[l_k c_k V_k\cos\phi_k + t_k\bar{c}_k[V]_k\cos\bar{\phi}_k] \quad (7)$$

where l_k is the length of the block base, t_k is the length of the interface between blocks k and $k-1$, bars denote material parameters on that interface, and velocities V_k and $[V]_k$ are as given in equations (5). Introducing c_d, ϕ_d, $\bar{c}_d$ and $\bar{\phi}_d$ (see equation (3)) into equation (6) and (7), and putting $\dot{D} = \dot{W}_\gamma$ so that a fictitious slope with parameters c_d, ϕ_d, $\bar{c}_d$, and $\bar{\phi}_d$ is on the verge of collapse (limit state), gives the factor of safety for the slope with non-zero cohesion

$$F = \frac{\sum_{k=1}^{n}\{l_k c_k V_k\cos\phi_{dk} + t_k\bar{c}_k[V]_k\cos\bar{\phi}_{dk}\}}{\sum_{k=1}^{n}V_k(G_k+Q_k)\sin(\alpha_k-\phi_{dk})} \quad (8)$$

where $\phi_{dk} = \tan^{-1}(\tan\phi_k/F)$ and $\bar{\phi}_{dk} = \tan^{-1}(\tan\bar{\phi}_k/F)$; angles ϕ_{dk} and $\bar{\phi}_{dk}$ also need to be used in place of ϕ_k and $\bar{\phi}_k$ when velocities are calculated from equation (5). The factor of safety F is applied to the strength of the soil along both the failure surface ABCD and the sliding surfaces between the blocks. The solution to the factor of safety is independent of the (arbitrarily assumed) velocity boundary condition V_0, as all the velocities are homogeneous first-order functions of V_0.

When $c_k = \bar{c}_k = 0$ and the associative flow rule holds, the dissipation rate $\dot{D} = 0$, and the energy balance during failure requires that $\dot{W}_\gamma = 0$. F in equation (8) then becomes indeterminate. The factor of safety can be calculated iteratively in such a case by requiring that $\dot{W}_\gamma$ in equation (6) (or the denominator in equation (8)) be equal to zero, where internal friction angle ϕ is replaced by $\phi_d = \tan^{-1}(\tan\phi/F)$. For a slope with a single inclination (and $c = 0$), the trivial solution to the safety factor is obtained when the rupture surface approaches the slope face: $F = \tan\phi/\tan\beta$, where β is the slope angle.

Consider a simple case where the soil strength on vertical block interfaces is neglected ($\bar{c}_k = 0$, $\bar{\phi}_k = 0$). The velocities of the blocks assume a simple form (Fig. 2(b))

$$V_k = V_0\frac{\cot(\alpha_1-\phi_1)}{\cos(\alpha_k-\phi_k)} \quad (9)$$

Velocities $[V]_k$ are irrelevant, as no energy is dissipated on vertical interfaces. Substituting equation (9) into equation (8) gives an expression for the factor of safety where the velocities are eliminated

$$F = \frac{\sum_{k=1}^{n}\dfrac{l_k c_k}{\cos\alpha_k+\sin\alpha_k(\tan\phi_k)/F}}{\sum_{k=1}^{n}(G_k+Q_k)\dfrac{\tan\alpha_k-(\tan\phi_k)/F}{1+\tan\alpha_k(\tan\phi_k)/F}} \quad (10)$$

The procedure of calculating the safety factor when $c = 0$ is the same as that already described.

PORE PRESSURE EFFECTS

The effect of the pore pressure can be included in the energy balance through terms due to seepage and buoyancy forces. It is now shown that the work of pore pressure on the expansion of the skeleton in a fully drained process is equivalent to the effect of buoyancy and seepage forces. The rate of work of pore water pressure on skeleton expansion is

$$\int_v u\dot{\varepsilon}_{ii}\,dv = \int_\Omega u\dot{\varepsilon}_{ii}\,d\Omega + \int_L un_i[V]_i\,dL \tag{11}$$

where u is the pore pressure, $\dot{\varepsilon}_{ii}$ is the volumetric deformation rate of the skeleton structure, $[V]_i$ is the velocity jump vector at velocity discontinuities, v is the volume of the submerged soil mass, and n_i is the unit vector normal to velocity discontinuity surfaces L. Velocity discontinuities L are included in volume v, and region Ω includes all the continually deforming subvolumes separated by discontinuities L. The first term in equation (11) represents the work of the pore pressure on the skeleton expansion in the continually deforming field only; the second term represents the work along discontinuities L.

The work rate expressed in equation (11) is positive work analogous to the work performed by a compressed fluid contained in a balloon, on virtual expansion of the balloon shell. Miller & Hamilton (1989) used a similar term to account for pore pressure effects in the analysis of a slope failure. While the technique they suggested gives correct numerical results, their interpretation of the pore pressure work as negative energy dissipation is disputable (Miller & Hamilton, 1990).

Using the Gauss theorem, the work rate of the pore water pressure for the entire domain (submerged volume) v can be written as

$$\int_v u\dot{\varepsilon}_{ii}\,dv = \int_v \frac{\partial}{\partial x_i}(uV_i)\,dv - \int_v \frac{\partial u}{\partial x_i}V_i\,dv$$

$$= \int_s un_i V_i\,dS - \int_v \frac{\partial u}{\partial x_i}V_i\,dv \tag{12}$$

where S is a surface bounding volume v and n_i is a unit vector normal to that surface. The hydraulic head h (with the omission of the kinetic part) is

$$h = (u/\gamma_w) + Z \tag{13}$$

where γ_w is the unit weight of water and Z is the elevation head. Substituting u from equation (13) into equation (12) gives

$$\int_v u\dot{\varepsilon}_{ii}\,dv = \int_s un_i V_i\,ds - \gamma_w \int_v \frac{\partial h}{\partial x_i}V_i\,dv + \gamma_w \int_v \frac{\partial Z}{\partial x_i}V_i\,dv \tag{14}$$

The first term on the right-hand side of equation (14) represents the work of the pore pressure on contour S of the submerged volume v. For a slope with a phreatic surface contained within the soil, this term is equal to zero. The second term denotes the work of the seepage force, and the third term is due to the force of buoyancy ($(\partial Z/\partial x_i)V_i = V_z$). To account for the effects of pore water pressure in a slope, one can explicitly include the seepage and buoyancy forces in the energy balance equation, or include the term on the left-hand side of equation (14) (see also equation (11)). The latter is done in the following analysis. In the present kinematic analysis the blocks are considered rigid, thus only the integral over discontinuities L in equation (11) contributes to the pore water pressure effect.

For an incompressible material such as clay ($\dot{\varepsilon}_{ii} = 0$) the net work of the pore pressure from equation (14) (or equation (11)) is zero, which indicates no influence of pore water pressure on the stability analysis.

FACTOR OF SAFETY IN THE PRESENCE OF PORE PRESSURE

The effect of pore pressure in the slope is included in the analysis using the pore water pressure work expressed in equation (11). The rate of energy due to the presence of pore water pressure in the slope collapsing according to the rigid-block mechanism as in Fig. 1(a) becomes

$$\dot{W}_u = \sum_{k=1}^{n} \{V_k l_k u_k \sin\phi_k + [V]_k t_k \bar{u}_k \sin\bar{\phi}_k\} \tag{15}$$

where u_k is the pore water pressure at the base of

$$F = \frac{\sum_{k=1}^{n} \{l_k c_k V_k \cos\phi_{dk} + t_k \bar{c}_k [V]_k \cos\bar{\phi}_{dk}\}}{\sum_{i=k}^{n} \{V_k[(G_k + Q_k)\sin(\alpha_k - \phi_{dk}) + l_k u_k \sin\phi_{dk}] + [V]_k t_k \bar{u}_k \sin\bar{\phi}_{dk}\}}$$

Fig. 3. Equation (16)

$$F = \frac{\sum_{k=1}^{n} \dfrac{l_k c_k}{\cos \alpha_k + \sin \alpha_k \, (\tan \phi_k)/F}}{\sum_{k=1}^{h} \left[(G_k + Q_k) \dfrac{\tan \alpha_k - (\tan \phi_k)/F}{1 + \tan \alpha_k \, (\tan \phi_k)/F} + \dfrac{l_k u_k}{\sin \alpha_k + \cos \alpha_k (F/\tan \phi_k)} \right]}$$

Fig. 4. Equation (17)

block k, and $\bar{u}_k$ is the average pore pressure on interface t_k. Introducing c_d, ϕ_d, $\bar{c}_d$ and $\bar{\phi}_d$ into equations (6), (7) and (15), and putting $\dot{D} = \dot{W}_\gamma + \dot{W}_u$ gives equation (16) shown in Fig. 3.

Velocities V_k and $[V]_k$ are given in equation (5), and again angles ϕ_{dk} and $\bar{\phi}_{dk}$ need to be used in place of ϕ_k and $\bar{\phi}_k$ when velocities from equation (5) are calculated. The procedure for calculating the safety factor when $c = \bar{c} = 0$ is the same as that described for the case where $u = 0$. For the special case where $\bar{\phi} = 0$ and $\bar{c} = 0$, equation (16) can be transformed into equation (17) shown in Fig. 4.

ROTATIONAL FAILURE MODE

Stability of slopes based on a rotational failure mechanism was considered by Chen *et al.* (1969) and Chen & Giger (1971) using the upper bound approach of limit analysis. The rotational mechanism is the most efficient in the kinematical approach (Chen, 1975), and it leads to lower critical heights than translational mechanisms do. The solution from the analysis of the rotational mechanism is used here as a reference. Kinematical admissibility requires that the failure surface for a rigid rotation collapse be a log-spiral expressed by the equation

$$r = r_0 \exp \left[(\theta - \theta_0) \tan \phi \right] \tag{18}$$

where r is the radius of the spiral related to angle θ, and r_0 and θ_0 are the initial values (Fig. 5). Chen and his co-workers found the critical height of slopes and their solution can be presented as a dimensionless stability factor

$$\frac{\gamma H}{c} = \frac{H}{r_0} \frac{\exp \left[2(\theta_h - \theta_0) \tan \phi \right] - 1}{2 \tan \phi (f_1 - f_2 - f_3 - f_4)} \tag{19}$$

where H/r_0 and functions f_1 to f_4 depend on the variables θ_0, θ_h and β' (see Fig. 5), and are given by Chen (1975). H denotes the height of the slope, γ is the unit weight of the soil and c is the cohesion. An optimization scheme can be used to find the minimum of $\gamma H/c$, with θ_0, θ_h and β' being the variables. For a slope of a known height the rotational failure analysis can be alternatively formulated in terms of the factor of safety to yield

$$F = \frac{2(\theta_h - \theta_0) \tan \phi}{\ln \left[1 + 2 \dfrac{\gamma H}{c} \dfrac{r_0}{H} \tan \phi (f_1 - f_2 - f_3 - f_4) \right]} \tag{20}$$

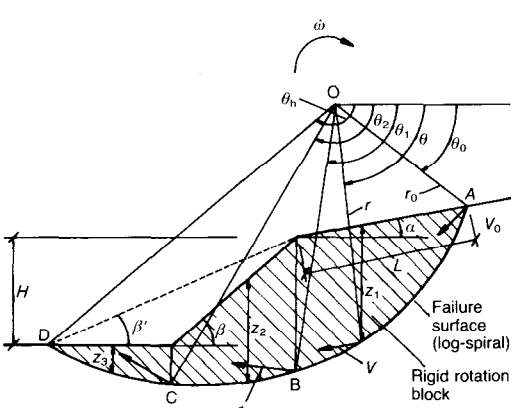

Fig. 5. Rotational failure mechanism for a homogeneous slope

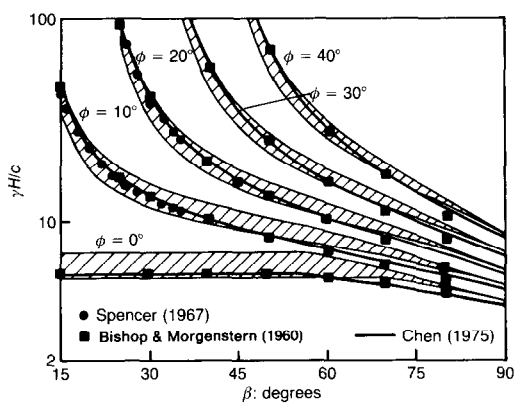

Fig. 6. Stability factor for homogeneous slopes with zero pore pressure: the shaded area represents the range of solutions for the translational mechanism ($r_u = 0$)

where $\gamma H/c$ is known, and H/r_0 and functions f_1 to f_4 need to be calculated using the same formulae as those in equation (19), but with tan ϕ replaced with tan ϕ/F. In the case where $\phi = 0$, the rule of de l'Hospital applied to equation (20) gives

$$F = \frac{H}{r_0} \frac{\theta_h - \theta_0}{\gamma H(f_1 - f_2 - f_3 - f_4)/c} \tag{21}$$

It is often stated that an analysis based on the rotational mechanism has two disadvantages: it becomes cumbersome when the soil is non-homogeneous, and no influence of the pore pressure is included (although an attempt for a specific case is presented by Miller & Hamilton, 1989). The influence of the pore pressure on the stability factor $\gamma H/c$ was obtained here by including work due to pore water pressure (equation (11)) on the right-hand side of equation (2) (not through seepage and buoyancy terms). The pore pressure is given here by coefficient r_u as described by Bishop & Morgenstern (1960). The stability coefficient takes a form very similar to that in equation (19)

$$\frac{\gamma H}{c} = \frac{H}{r_0} \frac{\exp\left[2(\theta_h - \theta_0)\tan\phi\right] - 1}{2\tan\phi(f_1 - f_2 - f_3 - f_4 + r_u f_5)} \tag{22}$$

where f_5 is a function of geometrical parameters and the internal friction angle (Appendix 1). The factor of safety now becomes

$$F = \frac{2(\theta_h - \theta_0)\tan\phi}{\ln\left[1 + 2\frac{\gamma H}{c}\frac{r_0}{H}\tan\phi(f_1 - f_2 - f_3 - f_4 + r_u f_5)\right]} \tag{23}$$

When $\phi = 0$, pore pressure has no influence on the result of the analysis as the work expressed in equation (11) (or equation (14)) is equal to zero.

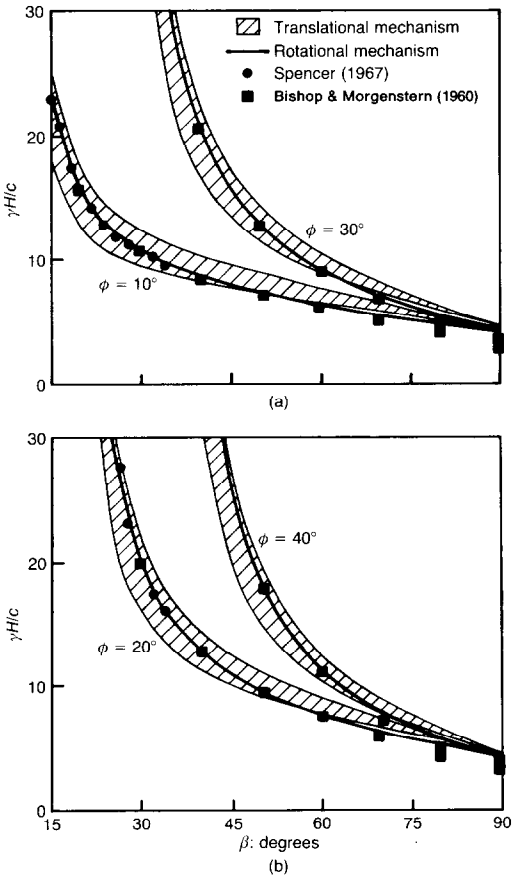

Fig. 7. Stability factor for homogeneous slopes and $r_u = 0{\cdot}25$

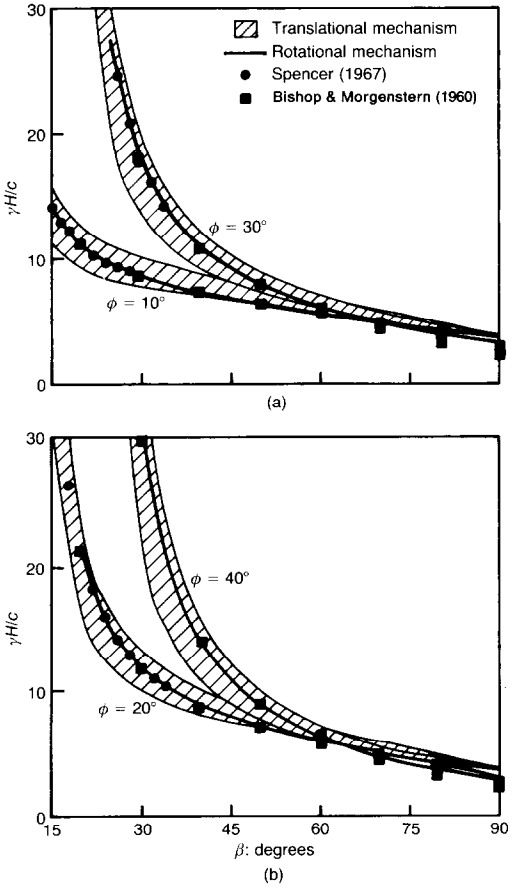

Fig. 8. Stability factor for homogeneous slopes and $r_u = 0{\cdot}5$

COMPUTATIONAL RESULTS

It is convenient to represent the results of calculations in terms of stability factor $\gamma H/c$ rather than the factor of safety for specific slopes. This factor, calculated for homogeneous slopes and using the translational and rotational collapse mechanisms, is shown in Figs 6–8. The pore pressure is expressed in terms of the coefficient r_u, and Figs. 6–8 represent results for r_u equal to 0, 0·25 and 0·5. Calculations were performed for β changing in 5° intervals. In addition, the results using the simplified Bishop method (Bishop & Morgenstern, 1960) are shown, as are the results given by Spencer (1967). All the results shown were calculated here except for those of Spencer (1967) and those for the rotational mechanism for $r_u = 0$ (Chen, 1975). In the presence of pore water pressure, there is a limit to the critical height of slopes with inclination angle slightly below the internal friction angle.

Calculations for the translational mechanism were performed assuming that the failure surface ABCD (Fig. 1(a)) follows the shape of a circular arc. The location of the circular arc is a function of three parameters that were considered variable in the minimization scheme where the minimum of $\gamma H/c$ was sought. The three variable parameters used in the analysis were the radius and the horizontal co-ordinates of points A and D (Fig. 1(a)). In the absence of pore-water pressure, stability factors increase rapidly with a drop in the slope angle; the results are shown in the semi-log plot (Fig. 6). The results for $r_u > 0$ are presented in a linear plot (Figs 7 and 8). The results for $\phi = 10°$ and 30° and for $\phi = 20°$ and 40° are presented on two separate diagrams for each $r_u > 0$. The shaded areas are bounded by the results from analyses of translational mechanisms for which the strengths on surfaces between the blocks were assumed to be equal to the actual strengths of the soil (upper curves), and for which the interslice strengths were neglected (lower curve). Increasing the strength of the soil anywhere in the slope cannot weaken the structure, and a drop in the soil strength cannot strengthen it. Hence, results for all combinations of $\bar{\phi}$ and $\bar{c}$ at interslice surfaces, which do not exceed the true values of ϕ and c for the soil, must be contained within the shaded areas. The upper curve for each internal friction angle is the strict upper bound to the stability factor $\gamma H/c$; the lower curve is an approximate solution. The two solutions become identical when the slope angle reaches 90°. This is because the most effective translational collapse mechanism for a 90° slope is one rigid block sliding over a planar failure surface; thus, the analysis becomes independent of interslice strength assumptions.

It can be argued that slice method solutions based on cylindrical failure surfaces, which fall above the range presented, either are non-minimal solutions to $\gamma H/c$ or imply that the strength on surfaces between blocks is larger than the actual strength of the soil. The solutions that fall below the range presented lead to the production of energy (thermodynamically inadmissible) when failure is interpreted as a translational collapse. This is true whether the technique uses one equation of slice equilibrium or three equations. It is evident from Figs 6–8 that the simplified Bishop analysis for steep slopes leads to an inadmissible production of energy when it is interpreted in the context of translational collapse.

The rigorous upper bound solution based on the rotational mechanism falls into the shaded region for slopes with an inclination angle less than about 50° (or greater, depending on ϕ and r_u). For very shallow slopes (small inclination angles) the rigorous upper bounds based on the two mechanisms (rotational and translational) become very close to each other. The solution based on the rotational mechanism, however, becomes significantly lower with an increase in the slope angle. For very steep slopes, this rigorous upper bound to $\gamma H/c$ drops below the shaded region which bounds all reasonable slice method solutions.

The results from the analysis using the simplified Bishop method follow the upper bound for the rotational collapse very closely, and drop below it only for very steep slopes. This is surprising, as the Bishop solution can be associated only with a translational mechanism (frictional soils with the normality rule), yet the results indicate good agreement with the upper bound solution based on the rotational mechanism. The solution by Spencer (1967) appears to follow this upper bound as closely as the Bishop analysis (for the range given by Spencer).

The influence of pore pressure is manifest by a reduction in stability factor $\gamma H/c$ with an increase in r_u (Figs 7 and 8). The adverse effect of the pore pressure depends on the magnitude of internal friction angle ϕ. When ϕ drops to zero, no adverse effect due to pore pressure is present. For a large pore pressure and steep slopes, $\gamma H/c$ does not increase with an increase in internal friction angle, as the increase in the adverse effect of the pore pressure exceeds the stabilizing effect due to an increase in ϕ. This is seen, for instance, in Fig. 8(b)), where the solutions for translational mechanisms (for $\phi = 20°$ and $\phi = 40°$) intersect. The same effect was noticed in the upper bound analysis based on the rotational mechanism, and in Bishop's simplified analysis.

Tables with stability factors for a wide range of parameters are presented by Michalowski (1995).

CONCLUSIONS

A stability analysis of slopes based on a translational mechanism of failure has been presented. A collapse mechanism was selected in the form of rigid blocks analogous to slices in traditional slice methods. This allows one to relate the proposed analysis to the traditional ones, and to assess the consequences of the static assumptions made in them. A convenient way to include pore pressure effects was presented and implemented. This technique for including pore pressure effects was also used here in analysis of rotational failures.

It was pointed out that an analysis based on the translational mechanism presented always satisfies the equations of equilibrium of forces. In this sense the result is equivalent to one that could be obtained from a limit equilibrium approach. All traditional slice methods are based on utilizing the latter. However, with the exception of Sarma (1979), the traditional slice techniques do not make an explicit assumption as to the yield condition on the interslice surfaces. Instead, to render the problem statically determinate, assumptions as to the location of the resultant force between the slices (thrust line) are made, or the inclination of these forces is assumed, and, in other cases, the interslice interactions are ignored. Assessment of these assumptions is not possible without reference to a more rigorous approach where at least a bound to the true limit load (critical height or safety factor) can be found.

After particular static assumptions are made in the traditional techniques of stability analyses (e.g. the location of the thrust line and the inclination of forces), the forces between the blocks (slices) can be calculated. When discussing these traditional analyses in view of the kinematically admissible failure mechanism, the interslice forces must be interpreted as the yield strength of the soil integrated over the surfaces between slices. This strength must be reached at the onset of failure in order to allow a relative movement of blocks. Rigid rotation without sliding within the moving soil mass is admissible only for log-spiral failure surfaces (cylindrical surfaces when $\phi = 0$). Differences among traditional analyses thus can be interpreted as making different assumptions for the soil strength between the slices.

In the kinematics-based method presented here, the strength of the soil between the blocks is assumed explicitly. This strength was taken here as zero, or as its maximum value set by the Mohr–Coulomb yield condition, and the results for all possible intermediate combinations of $\bar{\phi}$ and $\bar{c}$ are shown by the shaded areas in Figs 6–8. The assumptions made in the traditional slice methods can all be, in essence, reduced to postulating soil strength implicitly between the slices. For instance, the (constant) inclination of the interslice forces in the Spencer (1967) analysis for cohesionless soils can be interpreted as assuming a constant internal friction angle of the soil on these interfaces. Only if the strength of the soil on interfaces were assumed larger than the actual strength of the soil could a slice method solution give a stability factor $\gamma H/c$ higher than the upper limit of the shaded range in Figs 6–8. The solution below the lower limit of the shaded range would be possible (for a cylindrical failure surface) if a negative strength were assumed on some interfaces (physically inadmissible). In a kinematics-based solution such an assumption is equivalent to allowing negative dissipation, or the production of energy, on interfaces (thermodynamically inadmissible).

If traditional slice analyses are associated with kinematically admissible collapse mechanisms, then their solutions must fall in the shaded regions in Figs 6–8, irrespective of whether the method requires one, two or three equations of equilibrium to be satisfied for each slice. This is because the shaded areas include solutions for the interslice strength varied from zero to its maximum (the actual soil strength), which is equivalent to solutions by slice methods for all admissible combinations of interslice forces. Figs 6–8 show that the simplified Bishop analysis yields stability factors $\gamma H/c$ below the shaded range for very steep slopes. This indicates that forces associated with this solution would lead to the production of energy in at least some parts of the translational mechanism considered here. This theoretical inconsistency does not diminish the practical effectiveness of Bishop's method.

Of the two rigorous upper bounds to the critical height $\gamma H/c$, the one based on the rotational mechanism is better (lower). This is in accordance with the suggestion of Chen (1975) that the rotational one is the most effective of all admissible mechanisms. The simplified Bishop analysis based on the cylindrical failure surface follows this upper bound very closely (for all pore pressures), and becomes more conservative only for very steep slopes.

The solutions based on translational mechanisms satisfy the equilibrium equations of forces. As the failure mechanism does not include rotation, couples do no work during the failure process; consequently, moments become irrelevant in the analysis. The resultant forces on all block interfaces are uniquely determined from kinematical analysis, and can be calculated after the factor of safety (or critical height) is found. The location of the resultants on interslice surfaces can then be calculated from the moment equilibrium equations. If the thrust line is specified, as it is in some traditional slice methods, then the calculated interslice limit forces

(interpreted as integrated strength) indicate variation of strength on different interfaces. These forces and the force back-calculated from the method presented here are then different. None of the methods assures a statically admissible stress field and all must be considered approximate. The method presented here, however, makes it possible to bound the results (safety factors) from other slice techniques by performing calculations for two external assumptions (full strength or no strength on interfaces between slices).

A translational rigid-block mechanism can be associated with traditional slice techniques for slope stability analysis. Static assumptions made in these slice methods have the same consequences as postulating an arbitrary strength on surfaces between slices. All slice method solutions that can be associated with an admissible failure mechanism then fall into the range determined by two kinematics-based solutions: one where the interfacial strength is neglected, and the other where this strength is assumed equal to the actual strength of the soil. The latter is the rigorous upper bound to the factor of safety or the critical height of the slope. Traditional solutions that fall beyond the range indicated lead to unreasonable consequences when interpreted in view of the collapse mechanism.

Stability factors $\gamma H/c$ have been calculated using the method suggested based on the kinematical approach of limit analysis. Solutions for cylindrical failure surfaces are shown, but the analysis is valid for any shape. The analysis can be extended easily to non-homogeneous soils, with the conservative assumption that the internal friction angle of soil on surfaces between blocks does not exceed the internal friction angle of the weakest soil in the block.

In conservative analysis the strength of the soil is neglected on the interblock surfaces, but for steep slopes the analysis based on the rotational mechanism should be used, which yields even lower results despite being the strict upper bound to the true solution. The simplified Bishop (1955) method was found to be a very good approximation of the upper bound solution based on the rotational mechanism of failure both with and without pore pressure effects.

ACKNOWLEDGEMENT

The results presented in this Paper are based upon work supported by the National Science Foundation under grant MSS9301494. This support is gratefully acknowledged.

APPENDIX 1. ROTATIONAL FAILURE MECHANISM: PORE PRESSURE EFFECTS

The influence of pore pressure in the analysis based on the rotational failure mechanism is accounted for by including work of the pore pressure on the skeleton expansion during failure on the right-hand side of equation (2) (fully drained process). In a rigid rotation mechanism this work is performed along the log-spiral surface ABCD (Fig. 5). Pore pressure is represented here as

$$u = r_u \gamma z \tag{24}$$

where r_u is the pore pressure coefficient, γ is the unit weight of the soil and z is the vertical distance from the point on the slip surface to the slope surface (Bishop & Morgenstern, 1960). Distance z associated with section AB of the slip surface (Fig. 5) is denoted here by z_1, and z_2 and z_3 are related to sections BC and CD respectively. Angles θ_1 and θ_2 were found from

$$\cos\theta_1 \exp[(\theta_1 - \theta_0)] \tan\phi = \cos\theta_0 - \frac{L}{r_0}\cos\alpha$$

$$\cos\theta_2 \exp[(\theta_2 - \theta_0)\tan\phi] = \cos\theta_0 - \frac{L}{r_0}\cos\alpha - \frac{H}{r_0}\cot\beta \tag{25}$$

where L/r_0 and H/r_0 are given by Chen (1975) and all symbols are shown in Fig. 5. For toe failures θ_2 is equal to θ_h. Expressions for z_1, z_2 and z_3 can be written as

$$\frac{z_1}{r_0} = \frac{r}{r_0}\sin\theta - \sin\theta_0 - \left(\cos\theta_0 - \frac{r}{r_0}\cos\theta\right)\tan\alpha$$

$$\frac{z_2}{r_0} = \frac{r}{r_0}\sin\theta - \sin\theta_h \exp[\theta_h - \theta_0)\tan\phi] + \left(\frac{r}{r_0}\cos\theta - \cos\theta_2 \exp[(\theta_2 - \theta_0)\tan\phi]\right)\tan\beta$$

$$\frac{z_3}{r_0} = \frac{r}{r_0}\sin\theta - \sin\theta_h \exp[(\theta_h - \theta_0)\tan\phi] \tag{26}$$

where r is as described in equation (18). The work due to pore pressure along failure surface ABCD in the incipient failure with the rotation rate $\dot{\omega}$ about point O is

$$\dot{W}_u = \int_{\theta_0}^{\theta_h} u V_i n_i \frac{r}{\cos\phi}\,d\theta \tag{27}$$

where u is the pore pressure, V_i is the velocity jump vector along the failure surface, n_i is the unit vector normal to this surface and r is the radius of the spiral (equation (18)). A velocity jump vector along the log-spiral discontinuity in a kinematically admissible rigid rotation mechanism must propagate according to

$$V = V_0 \exp[(\theta - \theta_0)\tan\phi] = r_0\dot{\omega}\exp[(\theta - \theta_0)\tan\phi] \tag{28}$$

Equation (27) can now be written as

$$\dot{W}_u = \gamma r_0^2\, \dot{\omega} r_u \tan\phi \left(\int_{\theta_0}^{\theta_1} z_1 \exp\left[2(\theta - \theta_0)\tan\phi\right] \mathrm{d}\theta + \int_{\theta_1}^{\theta_2} z_2 \exp\left[2(\theta - \theta_0)\tan\phi\right] \mathrm{d}\theta + \int_{\theta_2}^{\theta_b} z_3 \exp\left[2(\theta - \theta_0)\tan\phi\right] \mathrm{d}\theta \right) \tag{29}$$

where z_1, z_2 and z_3 are as given in equations (26). The third integral in equation (29) is equal to zero for toe failures. Analytical solutions were found for integrals in equation (29). Equation (29) can be rewritten as

$$\dot{W}_u = \gamma r_0^3\, \dot{\omega} r_u \mathrm{f}_5 \tag{30}$$

where f_5 is the coefficient dependent on the geometrical parameters and ϕ. Coefficient f_5 is used in equation (22) for calculations of the stability factor $\gamma H/c$.

NOTATION

- c cohesion
- $\bar{c}$ cohesion at surfaces between blocks
- d energy dissipation rate per unit surface
- $\dot{D}$ total energy dissipation rate in the collapse mechanism during incipient failure
- f_i geometric functions ($i = 1$–5)
- F factor of safety
- h hydraulic head
- H height of slope
- l_k length of the block base
- n number of blocks in collapse mechanism
- $\boldsymbol{n}_i$ unit vector
- r radius of log-spiral
- r_u pore pressure coefficient
- t_k height of interface between blocks k and $k-1$
- u pore pressure
- $\boldsymbol{V}_i$ velocity vector
- V_k magnitude of velocity of kth block
- $[V]_k$ magnitude of velocity jump between blocks k and $k-1$
- $\dot{W}_u$ work rate due to pore water pressure
- $\dot{W}_\gamma$ work rate of gravity forces and tractions
- Z elevation head
- α_k inclination of the block base
- β slope angle
- γ unit weight of soil
- γ_w unit weight of water
- $\dot{\varepsilon}_{ij}$ skeleton strain rate tensor
- θ angle (variable)
- σ_{ij}' effective stress tensor
- ϕ internal friction angle
- $\bar{\phi}$ internal friction angle at surfaces between blocks

REFERENCES

Bishop, A. W. (1955). The use of slip circle in the stability analysis of slopes. *Géotechnique* **5,** No. 1, 7–17.

Bishop, A. W. & Morgenstern, N. R. (1960). Stability coefficients for earth slopes. *Géotechnique* **10,** No. 4, 129–150.

Chen, W. F. (1975). *Limit analysis and soil plasticity.* Amsterdam: Elsevier.

Chen, W. F. and Giger, M. W. (1971). Limit analysis of stability of slopes. *J. Soil Mech. Fdn Engng Am. Soc. Civ. Engrs* **97,** No. 1, 19–26.

Chen, W. F. and Giger, M. W. (1971). Limit analysis of stability of slopes. *J. Soil Mech. Fdn Engng Am. Soc. C4,* 23–32.

Drescher, A. (1991). *Analytical methods in bin-loads analysis.* Amsterdam: Elsevier.

Drescher, A. & Detournay, E. (1993). Limit load in translational failure mechanisms for associative and non-associative materials. *Géotechnique* **43,** No. 3, 443–456.

Fellenius, W. (1927). *Erdstatische Berechnungen.* Berlin: Ernst.

Izbicki, R. J. (1981). Limit plasticity approach to slope stability problems. *J. Geotech. Engng Div. Am. Soc. Civ. Engrs* **107,** No. 2, 228–233.

Janbu, N. (1957). Earth pressures and bearing capacity calculations by generalized procedure by slices. *Proc. 4th Int. Conf. Soil Mech., London* **2,** 207–212.

Janbu, N. (1973). Slope stability computations. *Embankment-dam engineering,* Casagrande volume, (eds R. C. Hirschfeld & S. J. Poulos). New York: Wiley.

Janssen, H. A. (1895). Verusche über Getreidedruck in Silozellen. *Z. Ver. Dsch Ing.* **39,** 1045–1049.

Karal, K. (1977). Energy method for soil stability analyses. *J. Geotech Engng Div. Am. Soc. Civ. Engrs* **103,** No. 5, 431–445.

Michalowski, R. L. (1984). A differential slice approach to the probelm of retaining wall loading. *Int. J. Numer. Anal. Meth. Geomech.* **8,** No. 4, 493–502.

Michalowski, R. L. (1989). Three-dimensional analysis of locally loaded slopes. *Géotechnique* **39,** No. 1, 27–38.

Michalowski, R. L. (1995). Stability of slopes: limit analysis approach. *Rev. Engng Geol.* **10.**

Miller, T. W. & Hamilton, J. H. (1989). A new analysis procedure to explain a slope failure at the Martin Lake mine. *Géotechnique* **39,** No. 1, 107–123.

Miller, T. W. & Hamilton, J. H. (1990). Discussion on a new analysis procedure to explain a slope failure at the Martin Lake mine. *Géotechnique* **40,** No. 1, 145–147.

Morgenstern, N. R. & Price, V. E. (1965). The analysis of the stability of general slip surfaces. *Géotechnique* **15,** No. 1, 79–93.

Mróz, Z. & Drescher, A. (1969). Limit plasticity approach to some cases of flow of bulk solids. *J. Engng Ind. Trans. Am. Soc. Mech. Engrs* **51,** 357–364.

Sarma, S. K. (1979). Stability analysis of embankments and slopes. *J. Geotech. Engng Div. Am. Soc. Civ. Engrs* **105,** No. 12, 1511–1524.

Spencer, E. (1967). A method of analysis of the stability of embankments assuming parallel inter-slice forces. *Géotechnique* **17,** No. 1, 11–26.